Multiple nπ* Transitions in Tetramethyl-1,3-cyclobutanedione. I. Spectroscopic Assignments

R. Spafford, J. Baiardo, J. Wrobel, and M. Vala*

Contribution from the Department of Chemistry, University of Florida, Gainesville, Florida 32611. *Received December 31, 1975*

Abstract: The low-temperature, single-crystal, polarized absorption spectrum of the cyclic diketone tetramethyl-1,3-cyclobutanedione (TMCBD) has been investigated. Four different, resolved electronic singlet nπ* transitions have been observed. From an analysis of the vibrational structure, polarization behavior, and relative intensities the observed bands have been assigned to transitions to ^1A_u ($^1A_2$), $^1B_{2g}$ (^1B_g), $^1B_{2g}$ ($^1B_1$), and ^1A_u (^1A_u) states (in order of increasing energy). Evidence is presented which shows that all four nπ* excited states are distorted: the first and third to a C_{2v} boat-like geometry and the second and fourth to a C_{2h} chair-like geometry; in all nπ* states the carbonyl groups are distorted to a pyramidal conformation. Three different mechanisms of intensity enhancement—vibronic mixing, valence distortion, and crystalline site effects—are discussed and shown to be operative in different regions.

I. Introduction

The interaction between nonbonding electron pairs in diketones is a subject of considerable current interest. Previous workers[1-4] have investigated the solution absorption spectroscopy of tetramethyl-1,3-cyclobutanedione (TMCBD), a cyclic diketone, and assigned two low intensity bands in the 250–370-nm region to two singlet nπ* transitions. The presence of two nπ* bands was attributed to the transannular interaction between the carbonyls' antibonding π* molecular orbitals causing a splitting into a π_+* and π_-* combination. Transitions to each of these orbitals was thought to occur from the noninteractive, degenerate carbonyl nonbonding orbitals. This view of the interaction between n orbitals and π* orbitals in diketones was generally held by workers in the field until 1970, when Swenson and Hoffmann[5] predicted from their EHT and CNDO/2 calculations that there should be a large interaction between the n orbitals of certain diketones as a result of a "through-bond" mechanism. Soon thereafter, Cowan et al.[6] measured the photoelectron spectrum of TMCBD, among other diketones, and showed that indeed there was a large separation between the n orbitals (0.7 eV). This large splitting was attributed to a "through-bond" interaction of the two carbonyl n orbitals. With this large n orbital splitting documented, we felt it was of interest to determine whether the two previously observed absorption bands in TMCBD were solely the result of this nonbonding orbital interaction or whether there was, in addition, an interaction between the π* orbitals which might lead to the observation of four nπ* bands. In this paper (hereafter called I), we outline briefly the results of our low-temperature, polarized absorption spectrum of single-crystal TMCBD in the singlet nπ* region and present evidence for the existence of four separate and distinct nπ* transitions. The electronic symmetry assignments of each of these four transitions are given and the mechanisms of intensity enhancement (crystalline site, vibronic interaction, and valence distortion) discussed. In the paper immediately following (II), we use these assignments and the observed spectral splittings to discuss the existence of "through-bond" interactions which influence both nonbonding and antibonding π orbital splittings. We also point out that the extended Hückel theory is superior to the CNDO/S semiempirical method in predicting the energies and relative ordering of the singlet nπ* states and discuss some of the reasons for its better performance. Previous studies on the vibrational spectra,[8] the vacuum ultraviolet spectra,[9] and the low-temperature crystal triplet spectrum[10] of TMCBD have recently been reported.

II. Crystallographic Data

The crystal structure of TMCBD is relatively simple[7] and the orientation of the molecules in the unit cell favorable for a single crystal polarized absorption spectral study. Figure 1 shows the alignment of the TMCBD molecules in the monoclinic unit cell. The cyclobutanedione backbone is planar (D_{2h} symmetry) and lies in the *ac* plane, such that the dicarbonyl axis is exactly perpendicular to the *b* axis. Absorption of radiation polarized parallel and perpendicular to the *b* axis will, therefore, directly reveal out-of-plane and in-plane transitions, respectively. Since there is only one molecule in the primitive unit cell, there is no possibility of Davydov exciton splitting complicating our polarization results. The crystal factor and site groups are both C_{2h}.

III. Experimental Section

TMCBD was obtained from Aldrich Chemical Co. and was purified by recrystallization from benzene or toluene. Thin single crystals with the *ab* face predominant were readily grown by slow solvent evaporation at room temperature. Orthoscopic examination and x-ray diffraction were used to align the crystals. The monoclinic *b* axis is easily identified in the *ab* face as lying perpendicular to that crystal edge which is parallel to an extinction direction. Survey spectra were run on Cary 14 and 17 uv-visible spectrophotometers using Glan-Thompson polarizers. For these spectra, samples were mounted on the cold finger of a liquid helium dewar; the temperature as measured by a copper-constantan thermocouple was ~20 K. More detailed, higher resolution spectra were run at 4.2 K on a 2 m Jena spectrograph or at 1.8 K on a 1 m Huet spectrograph. A Wollaston polarizer was used together with Kodak 103a0 spectral plates or Ilford N-40 plates.

IV. Spectral Results

A. Solution Absorption Spectra. Figure 2 shows the solution spectrum of TMCBD in isooctane and in ethanol at room temperature. There is a blue shift for all the bands in ethanol which together with their low intensities strongly supports the assignment of these bands to nπ* transitions. This conclusion was initially reached by Kosower[2] who assigned the two prominent peaks to two nπ* transitions resulting from the transannular interaction of the carbonyls' π* orbitals.

B. Single Crystal Polarized Absorption Spectra. Figure 3 shows an overall view of the 20 K single crystal, polarized absorption spectra of TMCBD. Detailed views of different sections at lower temperatures and higher resolution are given in Figures 4-6. The striking features of these spectra include: (1) four bands with apparent origins at 368.8, 332.0, 312.0, and

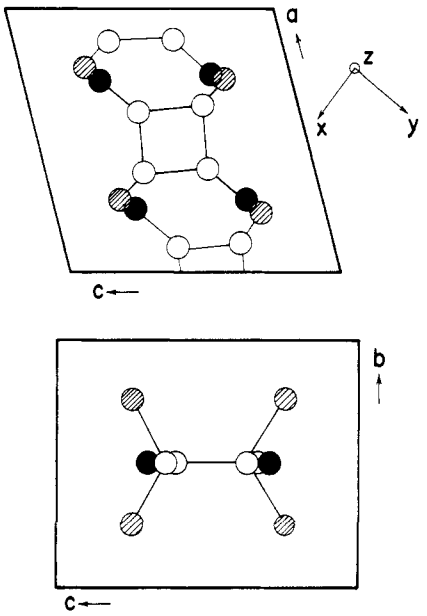

Figure 1. Top: Projection of TMCBD molecules on the *ac* plane. The *b* monoclinic axis is perpendicular to this plane. Bottom: Projection of TMCBD molecules on the *bc* plane. The slant-lined circles represent methyl groups, the solid black circles oxygen atoms, and the open circles carbon atoms (adapted from ref 7a).

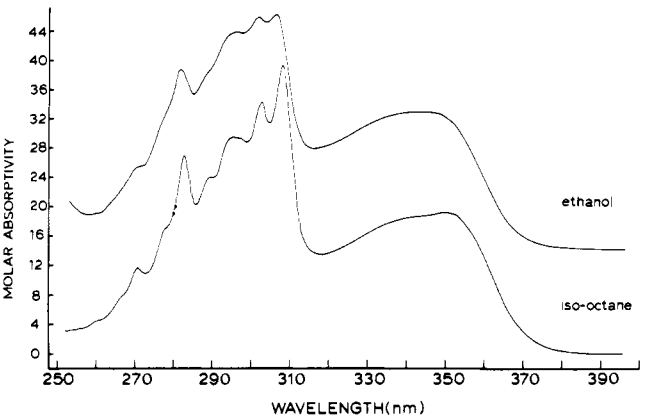

Figure 2. Solution spectrum of TMCBD in ethanol and isooctane at room temperature. The spectrum in ethanol has been vertically displaced 14 molar absorptivity units for clarity.

284.8 nm; (2) the first band origin (368.8 nm) is solely out-of-plane (z) polarized, the second band origin (332.0 nm) is both in-plane (xy) and out-of-plane polarized, the third band origin (312.0 nm) is z polarized, and the fourth origin (285.1 nm) parallels the second and is xy and z polarized; (3) the first two bands display much sharper vibrational structure than the higher energy two and contain long progressions in a 308-cm^{-1} vibrational mode. The third and fourth bands are not further resolved by lowering the temperature to 1.8 K; they remain as shown in the 20 K spectrum (Figure 3).

(1) **370-nm Band.** The detailed view of this band at 1.8 K (Figure 4) reveals the presence of three easily discernible progressions in a 308-cm^{-1} vibrational mode in the z polarization: one commencing on the 368.8-nm origin, the second on a 520-cm^{-1} vibronic origin, and the third on a 1039-cm^{-1} vibronic origin (2×520 cm^{-1}). The 368.8-nm origin is almost certainly the electronic origin (0-0 transition) of this band. We have measured the spectrum at 1.8 K in this region on crystals up to 1.0-cm thick where we have clearly seen the singlet-triplet transition lying just below this origin. We have observed no lines to the red of the 368.8-nm origin which could not be

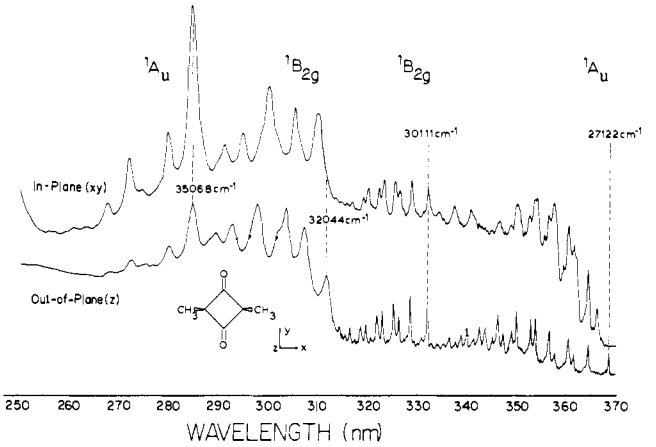

Figure 3. Single crystal polarized absorption spectrum of TMCBD on a (001) face at 20 K.

assigned to the triplet state. The out-of-plane polarization is comprised exclusively of bands belonging to these three progressions, whereas the in-plane polarization appears more complicated and contains at least three strong vibrational frequencies (189, 245, and 326 cm^{-1}) which are vibronic origins. To obtain more information on the polarization (x or y) of these vibronic origins, polarized spectra were recorded with radiation incident on the *ac* face (the plane to which the molecular backbone is parallel) and polarized parallel and perpendicular to the extinction direction. That this process resulted in true polarizations along the x and y axes of the TMCBD molecule is confirmed by the following observation. For a similarly aligned crystal, the singlet–triplet absorption, which was previously observed[10] to be completely in-plane (xy) polarized when irradiated on its *ab* face, was now seen to be exclusively y polarized, i.e., in-plane parallel to the carbonyl axis. This transition moment orientation has been observed for other carbonyl $n\pi^*$ triplets also.

The results of the *ac* face measurements are shown in Figure 5 for the lower energy region of the first band. Both the 189-cm^{-1} and the 245-cm^{-1} bands are predominantly x polarized while the 326-cm^{-1} band is predominantly y polarized.

(2) **332-nm Band.** The second band origin is displaced ~3000 cm^{-1} from the first band origin and, unlike any of the bands in the first transition, is both xy and z polarized, with the former polarization more intense than the latter. Three simple progressions in a 308-cm^{-1} mode are observed (Figure 4), the first starting at the 332.0-nm origin band and the other two starting on successive members of a 526-cm^{-1} vibration. Every band in this transition is xy and z polarized; no extra vibronic origins appear in the in-plane polarization.

(3) **312-nm Band.** The overall appearance of this band is very different from the two preceding ones: its component bands are intrinsically broader, the overall band intensity is somewhat greater, and the vibrational structure is not dominated by the 308-cm^{-1} progressions. A progression in a 490-cm^{-1} mode is evident in the out-of-plane polarization (see Figure 6). The origin band is z polarized and the remainder of the bands alternate in polarization. At 1.8 K, the broad origin band of this transition is overlapped by the sharp vibrational bands from the lower 332.0-nm band.

(4) **285-nm Band.** Although more closely resembling the third transition with its broad vibrational structure than the first two, this band is also distinct in two respects: the origin band is xy and z polarized, and its Franck-Condon vibrational envelope has the appearance of an allowed transition with the first vibrational component most intense. Because of the broadness of the vibrational bands, an analysis is difficult; however, a two-membered 1584-cm^{-1} mode progression upon

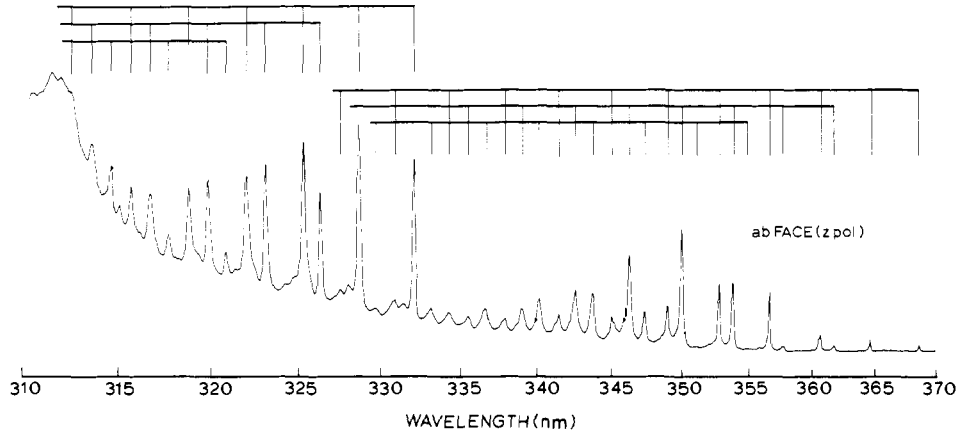

Figure 4. Out-of-plane single crystal polarized absorption spectrum of TMCBD on (001) face at 1.8 K in the region of the two lowest singlet $n\pi^*$ transitions.

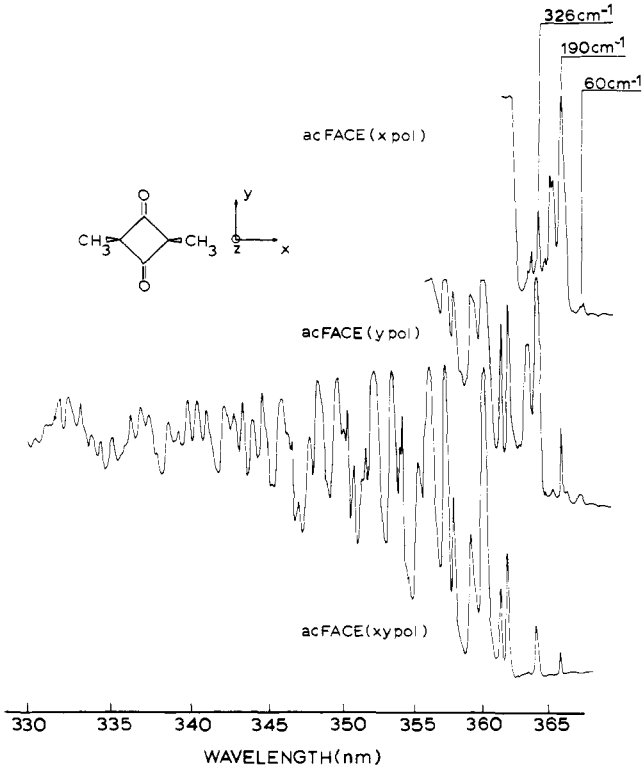

Figure 5. In-plane polarized single crystal absorption spectra of TMCBD on (010) face at 1.8 K in the region of the lowest singlet $n\pi^*$ transition. The lower (xy) spectrum is unpolarized and from a different crystal than upper two polarized spectra.

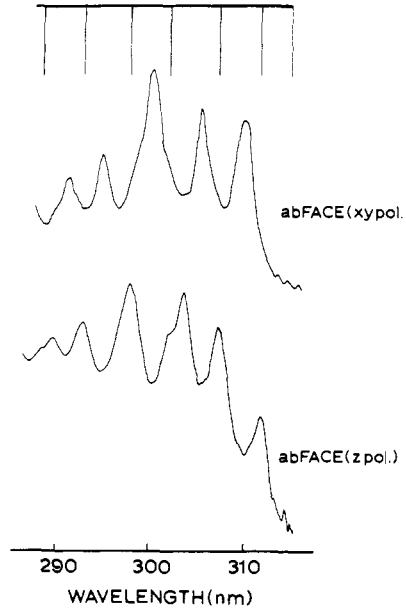

Figure 6. Polarized absorption spectra of single crystal TMCBD on the (001) face at 20 K in the region of the third singlet $n\pi^*$ transition.

each member of which are built 602-cm^{-1} and 1238-cm^{-1} vibrations is apparent.

C. Search for Low-Temperature Luminescence. It has been reported[11] that TMCBD does not fluoresce or phosphoresce in an EPA (ethanol-isopentane-ether) glass at 77 K. We have searched for the luminescence from single crystal TMCBD at 10 K using photoelectric detection, but with no success. Presumably, the energy dissipation pathways including photodegradation to dimethylketene followed by subsequent recombination to the dione are operative in the solid state also. In our initial absorption measurements, we did notice that the spectral resolution was markedly decreased for older crystals. Consequently, fresh crystals were used in all subsequent runs.

V. Vibrational Assignments in Ground Electronic State

The successful interpretation of the low-temperature absorption spectra hinges in large measure on the assignment of particular vibrational frequencies to their correct symmetry species. Previous work[8] on the vapor, solution, and solid state ir and Raman spectra of TMCBD was successful in assigning a number of vibrations and in narrowing the possible symmetry choices in the remaining ones. The results of this work for the low-energy vibrational frequencies important to this investigation are listed in the first two columns in Table I. Only the frequencies which involve the cyclobutane ring and the carbonyl groups have been included in the table since they are the most likely ones to be excited in an $n\pi^*$ transition. Several band symmetries in the table are given in quotes since it was not possible to pinpoint the symmetry further by experimental means; e.g., a "b_u" designation means the vibration could be either b_{1u}, b_{2u}, or b_{3u}.

Since we are primarily interested in carbonyl and ring modes, it is a simple matter to determine the number and types of various modes. For cyclobutanedione (neglecting the hydrogens) and for cyclobutane (in parentheses) the various symmetries and number of modes of that symmetry are: a_{1g}: 3(2), b_{1g}:2(1), b_{3g}:1(0), b_{1u}:2(1), b_{2u}:2(1), and b_{3u}:2(1). Thus, vibrations involving the carbonyl group include one of each of these symmetries. The probable vibrational motions are: a_{1g}, symmetric carbonyl stretch; b_{1g}, out-of-phase in-plane carbonyl bend; b_{3g}, out-of-phase carbonyl wag; b_{1u}, in-phase out-of-plane wag; b_{2u}, asymmetric carbonyl stretch; b_{3u}, in-

Table I. Vibrational Frequencies and Symmetry Assignments for Crystalline Tetramethyl-1,3-cyclobutanedione

Obsd frequency,[a,b] cm^{-1}	Experimental symmetry[b]	Assignment	Type of vibration
82, m (ir)	b_{1u}	b_{1u}	Ring puckering
162, vs (R)	b_{2g}/b_{3g}	b_{3g}	Out-of-plane carbonyl wag
186, s (ir)	b_{3u}/b_{1u}	b_{3u}	In-plane ring distortion
216, m (R)	a_g/b_{1g}	b_{1g}	In-plane carbonyl bend
270, w (R)	"b_g"	b_{2g}	Combination (b_{1u} (82) + b_{3u} (186))
286, s (ir)	b_{3u}/b_{1u}	b_{3u}	In-plane carbonyl bend
298, s (R)	a_g	a_g	Ring distortion
402, m (ir)	"b_u"	b_{1u}	Out-of-plane carbonyl wag
589, m (R)	a_g	a_g	CH_3 mode (ring breathing?)
637, vs (R)	a_g	a_g	Ring breathing (CH_3 mode?)
661, w (R)	b_{1g}	b_{1g}	Ring distortion
764, m (ir)	"b_u"	b_{2u}	In-plane ring distortion
818, m (ir)	b_{1u}/b_{3u}	b_{1u}/b_{3u}	Methyl mode?
1748, vs (ir)	b_{2u}	b_{2u}	Asymmetric carbonyl stretch
1847, w (R)	a_g	a_g	Symmetric carbonyl stretch

[a] w = weak, m = medium, s = strong, vs = very strong; R = Raman, ir = infrared. [b] From ref 8.

Table II. Correlation Diagram for TMCBD Planar and Distorted Molecular (Boat-Form) Point Groups, Site Group, and Crystal Factor Group

D_{2h} (molecular point group)	C_{2v} (distorted molecular point group)	C_2 (site group)[a]	C_{2h} (crystal factor group)
A_g	A_1 (z)	A (z)	A_g
B_{1g}	A_2		B_g
B_{2g}			
B_{3g}			
A_u	$B_1(x)$	B (x,y)	A_u (z)
B_{1u} (z)	B_2 (y)		B_u (x,y)
B_{2u} (y)			
B_{3u} (x)			

[a] The site group is here taken to contain only those elements common to the new distorted molecular point symmetry and the unchanged crystal factor group.

Table III. Correlation Diagram for TMCBD Planar Point Group, Site Group, and Crystal Factor Group

D_{2h} (molecular point group)	C_{2h} (site group)	C_{2h} (crystal factor group)
A_g	A_g	A_g
B_{1g}		
B_{2g}	B_g	B_g
B_{3g}		
A_u	A_u (z)	A_u (z)
B_{1u} (z)		
B_{2u} (y)	B_u (x,y)	B_u (x,y)
B_{3u} (x)		

phase in-plane carbonyl bend. Several of these modes have already been unambiguously assigned as carbonyl stretching modes (1748 and 1847 cm^{-1}). Of the remaining carbonyl infrared bands, we assign the 402-cm^{-1} one to the b_{1u} carbonyl wag and the 286-cm^{-1} mode to the b_{3u} in-plane carbonyl bend, although an interchange of these two assignments would not affect our later conclusions. The remaining ir bands are assigned to various ring modes. The 82-cm^{-1} mode has been assigned[8] to the b_{1u} ring puckering mode.

For the gerade bands the two possible b_{1g} vibrations at 216 and 661 cm^{-1} are assigned to an in-plane CO bend and a ring distortion, respectively, the 162-cm^{-1} vibration to the b_{3g} out-of-plane carbonyl wag and the weak 270-cm^{-1} mode to a combination band: b_{1u} (82 cm^{-1}) + b_{3u} (186 cm^{-1}) = b_{2g} (268 cm^{-1}). The three remaining a_g modes, 298, 589, and 637 cm^{-1}, are assigned to the ring distortion mode, a methyl deformation mode, and a ring breathing mode, respectively, although the latter two could be interchanged.

VI. Excited State Assignments

Interaction of the carbonyl n orbitals (n_1 and n_2) leads to the first-order molecular orbitals:

$$n_+(b_{3u}) = (n_1 + n_2)/\sqrt{2}$$

$$n_-(b_{1g}) = (n_1 - n_2)/\sqrt{2}$$

with the indicated (D_{2h} group) symmetries. Similarly, interaction of the carbonyls' π^* orbitals (π_1^* and π_2^*) gives:

$$\pi_+^*(b_{1u}) = (\pi_1^* + \pi_2^*)/\sqrt{2}$$

$$\pi_-^*(b_{3g}) = (\pi_1^* - \pi_2^*)/\sqrt{2}$$

Two excited electronic states of symmetry ^1A_u and two of $^1B_{2g}$ result from electronic excitation between these sets of orbitals. Transitions to each of these states is symmetry forbidden (in D_{2h}).

A. 370-nm Band System. The assignment of the observed bands to the four possible $n\pi^*$ transitions is facilitated by an analysis of the vibrational structure and polarization behavior. For coupled carbonyl groups there are two kinds of CO wag: an in-phase b_{1u} and an out-of-phase b_{3g} mode. The 308-cm^{-1} vibration which forms long progressions in the first observed band is assigned to the b_{1u} out-of-plane in-phase carbonyl wag. In the ground state, this mode occurs at 402 cm^{-1}. Whitlock and Duncan[12] found the carbonyl out-of-plane wag in cyclobutanone at 394 cm^{-1} in the ground state and 317 cm^{-1} in the first excited ($n\pi^*$) singlet. The occurrence of long progressions in a non-totally symmetric mode usually indicates a distortion from planar D_{2h} symmetry in the excited state. It could be argued, following Table II, that the present vibrational and polarization observations are consistent only with a distortion to a boat (C_{2v}) conformation in which both carbonyls attain an in-phase pyramidal deformation. Transitions to a ^1A_u ($^1A_2$) state would then be allowed solely along the z direction because of crystalline site group effects. This conclusion is inconsistent, however, with the observation of a null Stark effect for this transition.[13] On the other hand, if the molecule were undergoing inversion via the carbonyl wagging vibration, the Stark result, the observation of long progressions in the CO wag, and the z polarization of the 0-0 band become understandable. The molecular force field experienced by the TMCBD molecule undergoing inversion is now D_{2h}. It can be seen in Table III that only for transitions to a ^1A_u $n\pi^*$ electronic state is a z-polarized electronic band possible; its intensity is induced via crystalline site effects and, thus, expected to be very weak, as observed. Further support for the ^1A_u assignment comes from the observed 1400-cm^{-1} interval to the lower ^3A_u $n\pi^*$ state,[10] a value characteristic of $n\pi^*$ singlet-triplet splittings.

A 308-cm^{-1} progression is also observed to be built on a vibronic origin at 520 and 1039 cm^{-1} (2 × 520 cm^{-1}). This vibration is assigned to a totally symmetric ring breathing mode which occurs at 637 cm^{-1} in the ground state.[8] In cyclobutanone the analogous mode was observed[12] at 670 cm^{-1} in the ground state and at 504 cm^{-1} in the $n'\pi^*$ state.

Table IV. Correlation Diagram for TMCBD Planar and Distorted Molecular (Symmetrical and Unsymmetrical Boat-Form) Point Groups

D_{2h} (molecular point group)	C_{2v} (distorted molecular point group)	C_s (distorted molecular point group)	C_1 (site group)
A_g	A_1 (z)	A' (y,z)	A (xyz)
B_{1g}	A_2		
B_{2g}			
B_{3g}	B_1 (x)	A'' (x)	
A_u			
B_{1u} (z)	B_2 (y)		
B_{2u} (y)			
B_{3u} (x)			

The first strong in-plane polarized band appears 189 cm^{-1} above the 0-0 band and is predominantly x polarized (perpendicular to the carbonyl axes). Its vibronic symmetry is therefore B_1 (in C_{2v}) which may originate from B_{2g} or B_{3u} in D_{2h}, indicating that the Herzberg-Teller active mode is either b_{2u} or b_{3g}. We assign the 189-cm^{-1} vibration to the b_{3g} carbonyl wag (162 cm^{-1} in the ground state) because the lowest lying b_{2u} mode, the in-plane ring distortion (cf. Table I) lies at much higher energies (764 cm^{-1}). It is not unexpected that the frequency of the b_{3g} carbonyl wag should increase in the $n\pi^*$ state since below the inversion barrier the ring strain is undoubtedly greater than in the ground state resulting in larger force constants for such motions.

The strong predominantly y-polarized band at 326 cm^{-1} has B_2 vibronic (C_{2v}) symmetry corresponding to either b_{3u} or b_{2g} (D_{2h}) vibronic mixing modes. Because the sole low-frequency b_{2g} mode is only a weak combination band, the 326-cm^{-1} mode is assigned to a b_{3u} vibration—most probably the ground state 286-cm^{-1} in-plane carbonyl bend.[8] The assignment of these two dominant vibrations to b_{3g} and b_{3u} (D_{2h}) symmetries dictates that their vibronic symmetries in the parent D_{2h} geometry be B_{3u} and B_{3g}, respectively (B_1 and B_2 in C_{2v}). Since transitions are allowed only to the former type state in D_{2h} but allowed to both B_1 and B_2 states in the true excited state C_{2v} geometry, it can be concluded that the in-plane intensity of this first transition is the result of both valence distortion and vibronic coupling to higher-lying (presumably $n\sigma^*$) transitions.[9] The vibrational analysis for the entire band system is given in Table V and Table VI.

The appearance of two low-frequency vibrations (62 and 81 cm^{-1}) above the 0-0 band presents something of an enigma. A low-frequency mode at 82 cm^{-1} was observed[8] in the ground state and assigned to the b_{1u} ring torsional mode. The appearance of such a mode in this electronic transition is predicted to appear only in the z polarization (cf. Table II) but the two observed bands are observed in the x and y polarizations with about equal intensity. Although several intriguing possible interpretations present themselves, we have no conclusive supporting evidence for either. The first possibility is that they represent transitions to the second triplet state of TMCBD and, second, the absorption of a small amount of dimethylketene photochemically formed and trapped in the TMCBD crystal lattice. The lowest triplet was observed[10] exclusively in-plane polarized, as are these bands. The energy spacing between two such triplets of ~1400 cm^{-1} is perhaps too small to be reasonable, however. Dimethylketene is a known photoproduct of TMCBD.[14] The fact that not all our spectra exhibited these bands tends to support this latter suggestion; further work is continuing on this point.

In summary, the 370-nm band is assigned to the $^1A_u(^1A_2) \leftarrow {}^1A_g$ transition in which the excited $n\pi^*$ state is distorted to a boat-like C_{2v} geometry with both carbonyls attaining a pyramidal conformation. The out-of-plane intensity is weak and solely site-symmetry induced while the in-plane intensity is stronger and induced both via valence distortion and Herzberg-Teller vibronic coupling to higher-lying states.

Table V. Vibrational Analysis of 370-nm Band System (z polarization)

Obsd frequency, cm^{-1}	Pol.	Obsd $\Delta\bar{\nu}$, cm^{-1}	Assignment, cm^{-1}	Calcd $\Delta\bar{\nu}$, cm^{-1}	$\Delta(\Delta\nu)$, cm^{-1}
27122	z	0	0–0		
27435	z	313	308	308	+5
27647	z	525	520	520	+5
27739	z	617	2 × 308	616	+1
27948	z	826	520 + 308	828	−2
28042	z	920	3 × 308	924	−4
28161	z	1039	2 × 520	1040	−1
28248	z	1126	520 + (2 × 308)	1136	−10
28345	z	1223	4 × 308	1232	−9
28466	z	1344	(2 × 520) + 308	1348	−4
28555	z	1433	520 + (3 × 308)	1444	−11
28645	z	1523	5 × 308	1540	−17
28785	z	1663	(2 × 520) + (2 × 308)	1656	+7
28868	z	1746	520 + (4 × 308)	1752	−6
28965	z	1843	6 × 308	1848	−5
29078	z	1956	(2 × 520) + (3 × 308)	1964	−8
29180	z	2058	520 + (5 × 308)	2060	−2
29274	z	2152	7 × 308	2156	−4
29395	z	2273	(2 × 520) + (4 × 308)	2272	+1
29490	z	2368	520 + (5 × 308)	2368	0
29577	z	2455	8 × 308	2464	−9
29700	z	2578	(2 × 520) + (5 × 308)	2580	−2
29798	z	2676	520 + (7 × 308)	2676	0
29909	z	2787	9 × 308	2772	+15
30003	z	2881	(2 × 520) + (6 × 308)	2888	−7

B. 332-nm Band System. The main feature differentiating this transition from the lower energy one is its xy and z polarization of every band. The appearance of several carbonyl wagging progressions (~308 cm^{-1}), one of which is built on a 526-cm^{-1} ring breathing vibronic origin, is very similar to the lower energy band (Figure 4 and Table VII). A plot of the carbonyl wag vibrational quantum number vs. energy for each of the three 308-cm^{-1} progressions in the lower ^1A_u transition yields three parallel straight lines. Curiously, if a similar plot is made of the two 308-cm^{-1} progressions of the present transition, they are found to be collinear with two of the lower state lines. From these superimposed plots, it appeared that the progression beginning on the 0-0 band of the lower ^1A_u transition continued into the present region for a total of 15 308-cm^{-1} vibrations. This relation between the vibrational components of these two transitions led us to initially believe that the two were in fact only one electronic transition. Three observations argue against this hypothesis, however. First, the appearance of a 526-cm^{-1} mode built on the 332.0-nm apparent origin is consistent only with a new electronic (or vibronic) origin. It is inconceivable that such a mode should suddenly appear in the middle of a long 308-cm^{-1} progression. Second, if the 332.0-nm apparent origin were a vibronic origin built on the ^1A_u 0-0 band, its frequency would be unreasonably large (i.e., ~3000 cm^{-1}). The activation of a CH stretch in the methyl groups of ~3000 cm^{-1} is precluded in this transition since the π^* orbital to which the electronic transition occurs possesses a node across the ring through the methyl carbons (cf. paper II following). Third, the appearance of intensity in both xy and z polarizations for all bands in this transition when such is not observed in the lower band also argues for a new electronic transition.

Table VI. Vibrational Analysis of 370-nm Band System (*xy* Polarization)

Obsd frequency, cm^{-1}	Pol.	Obsd $\Delta\bar{\nu}$, cm^{-1}	Assignment, cm^{-1}	Calcd $\Delta\bar{\nu}$, cm^{-1}	$\Delta(\Delta\nu)$, cm^{-1}
(27122)[a]	*z*		0–0		
27184	*xy*	62	62	62	
27203	*xy*	81	81	81	
27277	*y*	155	155	155	
27311	*x*	189	189	189	
27367	*x*	245	245	245	
27382	*x*	260	260	260	
27412	*x*	290	290	290	
27448	*y*	326	326	326	
27490	*y*	368	368	368	
27508	*y*	386	386	386	
27586	*y*	464	155 + 398	463	+1
27616	*xy*	494	189 + 308	497	−3
27655	*xy*	533	245 + 308	553	−20
27708	*xy*	586	290 + 308	598	−12
27747	*xy*	625	326 + 308	634	−9
27824	*xy*	702	386 + 308	694	+8
(27889)	*xy*	767	155 + (2 × 308)	771	−4
27933	*xy*	811	189 + (2 × 308)	805	+6
27972	*xy*	850	245 + (2 × 308)	861	−11
28011	*xy*	889	260 + (2 × 308)	876	+13
28027	*xy*	905	290 + (2 × 308)	906	−1
28066	*xy*	944	326 + (2 × 308)	942	+2
28090 (sh)[b]	*xy*	968	—	968	
28129	*xy*	1007	386 + (2 × 308)	1002	+5
28193 (sh)	*xy*	1071	155 + (3 × 308)	1079	−8
28233	*xy*	1111	189 + (3 × 308)	1113	−2
28280	*xy*	1158	245 + (3 × 308)	1169	−11
28329	*xy*	1207	290 + (3 × 308)	1214	−7
28385	*xy*	1263	326 + (3 × 308)	1250	+13
28433 (sh)	*xy*	1311		1311	
28441	*xy*	1319	386 + (3 × 308)	1310	+9
28490	*xy*	1368	155 + (4 × 308)	1387	−19
28523	*xy*	1401	189 + (4 × 308)	1421	−20
28588	*xy*	1466	245 + (4 × 308)	1477	−11
28637 (sh)	*xy*	1515	260 + (4 × 308)	1492	+23
28662	*xy*	1540	290 + (4 × 308)	1522	+18
28686	*xy*	1564	326 + (4 × 308)	1558	+6
28732 (sh)	*xy*	1610		1610	
28744	*xy*	1622	386 + (4 × 308)	1618	+4
28760	*xy*	1638	1638		
28794 (sh)	*xy*	1672	155 + (5 × 308)	1695	−23
28860	*xy*	1738	189 + (5 × 308)	1729	+11
28893	*xy*	1771	245 + (5 × 308)	1785	−14
28977	*xy*	1855	290 + (5 × 308)	1830	+25
29002	*xy*	1880	326 + (5 × 308)	1866	+14
29053	*xy*	1931	386 + (5 × 308)	1926	+5
29104	*xy*	1982	155 + (6 × 308)	2003	−21
29156	*xy*	2034	189 + (5 × 308)	2037	−3
29206	*xy*	2084	245 + (6 × 308)	2093	−9
29309	*xy*	2187	326 + (6 × 308)	2174	+13
29360	*xy*	2238	386 + (6 × 308)	2234	+3
29412	*xy*	2290	155 + (7 × 308)	2311	−21
29464	*xy*	2342	189 + (7 × 308)	2345	−3
29516	*xy*	2394	245 + (7 × 308)	2401	−7
29577	*xy*	2455	290 + (7 × 308)	2446	+11
29612	*xy*	2490	326 + (7 × 308)	2482	+8
29674	*xy*	2552	386 + (7 × 308)	2542	+10
29718	*xy*	2596	155 + (8 × 308)	2619	−23
29824	*xy*	2702	245 + (8 × 308)	2709	−7
29878	*xy*	2756	290 + (8 × 308)	2754	+2
29923	*xy*	2801	326 + (8 × 308)	2790	+11
29976	*xy*	2854	386 + (8 × 308)	2850	+4
30048	*xy*	2926	155 + (9 × 308)	2927	−1

[a] Frequencies in parentheses not observed. [b] sh = shoulder.

Table VII. Vibrational Analysis of 332-nm Band System

Obsd frequency, cm^{-1}	Pol.	Obsd $\Delta\bar{\nu}$, cm^{-1}	Assignment cm^{-1}	Calcd $\Delta\bar{\nu}$, cm^{-1}	$\Delta(\Delta\nu)$, cm^{-1}
(29785)[a]			0–0		
30111	*xyz*	326	326	326	
30414	*xyz*	629	326 + 308	634	−5
30637	*xyz*	852	326 + 526	852	0
30732	*xyz*	947	326 + (2 × 308)	942	+5
30941	*xyz*	1156	326 + 526 + 308	1160	−4
31046	*xyz*	1261	326 + (3 × 308)	1250	+11
31162	*xyz*	1377	326 + (2 × 526)	1378	−1
31250	*xyz*	1465	326 + 526 + (2 × 308)	1468	−3
31358	*xyz*	1573	326 + (4 × 308)	1558	+15
31466	*xyz*	1681	326 + (2 × 526) + 308	1686	−5
31566	*xyz*	1781	326 + 526 + (3 × 308)	1776	+5
31656	*xyz*	1871	326 + (5 × 308)	1866	+5
31737	*xyz*	1952	326 + 1626	1952	0
31776	*xyz*	1991	326 + (2 × 526) + (2 × 308)	1994	−3
31867	*xyz*	2082	326 + 526 + (4 × 308)	2084	−2

[a] Frequency in parentheses not observed.

Table VIII. Correlation Diagram for TMCBD Planar and Distorted Molecular (Chair-Form) Point Groups, Site Groups, and Crystal Factor Groups

D_{2h} (molecular point group)	C_{2h} (distorted molecular point group)	C_i^z (site group)[a]	C_{2h} (crystal factor group)
A_g	A_g	A_g	A_g
B_{1g}			
B_{2g}	B_g		B_g
B_{3g}			
A_u	$A_u(x)$	$A_u(xyz)$	$A_u(z)$
$B_{1u}(z)$			
$B_{2u}(y)$	$B_u(y,z)$		$B_u(xy)$
$B_{3u}(x)$			

[a] See footnote, Table II.

The presence of several progressions in a 308-cm^{-1} mode again indicates a distortion in the excited state. In this case, however, a distortion to a C_{2v} boat-like form will not account for the observed *xy* and *z* polarization of every band in this region (Table II). Distortion to a chair-like C_{2h} geometry scrambles the *y* and *z* polarizations for B_{1u} and B_{2u} (D_{2h}) vibronic symmetries[15] (Table VIII), but such a distortion requires that the progression forming mode be the b_{3g} out-of-plane carbonyl wag. That a 308-cm^{-1} vibration should be assigned here to a b_{3g} vibration is perhaps not unreasonable, since the n orbital (n_+) involved in the transition is the same one as in the lower transition and the π_+^* orbital electron distribution is very similar to that of the π_-^* orbital (cf. paper II).

Further support for this assignment and for the excited state distortion comes from our polarized absorption measurements on the *ac* crystal face, where the *x* and *y* polarized transitions may be separated. All structured bands in this region were observed to be more strongly polarized in the *y* direction than in the *x* direction, as predicted for distortion to C_{2h} geometry (Table VIII). The weaker *x*-polarized component is site-symmetry induced. In addition to the structured features in this region, there is an underlying broad structureless component with intensity primarily along the *x* direction. This may represent transitions to the dissociative state(s) responsible for the known photodegradation of TMCBD to the dimethylketene.

The assignment of the electronic symmetry of this transition can now be made. Upon distortion, transitions to a ^1A_u state should be seen solely along *x* (Table VIII), whereas transitions to a $^1B_{2g}$ state should not be seen at all. The former choice is inconsistent with experiment since the intensity in this transition is polarized predominantly along *y* and *z*. The latter choice is preferred if it is (reasonably) assumed that the observed intensity is vibronically induced.

The most probable candidate to effect the vibronic coupling is a b_{3u} vibration (e.g., the 326-cm^{-1} carbonyl in-plane bend). As mentioned above, all bands in this region must be of either

B_{1u} or B_{2u} (D_{2h}) symmetry to explain the polarization data. For a B_{2g} electronic state, this implies active vibrations of b_{3u} or a_u symmetries. The only a_u vibration observed in the crystalline ir work is a very weak band at 875 cm^{-1} assigned to either a methyl bending mode or a carbon–carbon stretching mode. Thus, a vibronically active b_{3u} mode in a $^1B_{2g}$ electronic state is most probably responsible for the intensity enhancement in this region and the distribution of this intensity to both in-plane and out-of-plane polarizations results from the upper state distortion to a C_{2h} chair-like geometry.

C. 312-nm Band System. The appearance of this system is very different from either of the two lower electronic transitions. Sharp, well-resolved 308-cm^{-1} carbonyl wagging progressions are now replaced by a multi-membered progression (Table IX) in a broad 490-cm^{-1} mode which commences on the 312.0-nm *z*-polarized peak. The breadth of these vibrations is retained even down to 1.8 K. In order to assign the electronic symmetry of this transition it is informative to compare overall band intensities between the present and the first absorption systems (368.8-nm region). The present *z*-polarized intensity is comparable with the first band *xy*-polarized intensity, which gains oscillator strength primarily via a vibronic coupling mechanism. It is also much more intense than the first band *z*-polarized intensity, which is induced solely via crystalline site effects. From this observation, it is reasonable to expect that neither the out-of-plane nor the in-plane intensity of the present transition is induced solely via crystalline site effects, and that a vibronic coupling mechanism is the primary source of intensity enhancement (vide infra for arguments on a valence distortion mechanism).

Vibronic interaction via either a b_{3u} or a b_{1g} vibration in a $^1B_{2g}$ or a ^1A_u state, respectively, may account for the *z*-polarized band at 312.0 nm, although the former mode (an in-plane carbonyl bend at 326 cm^{-1} in the ground state) is favored since it has been observed to be vibronically active in both of the two lower electronic transitions, while the latter has not. The appearance of a band 189 cm^{-1} above the 312.0-nm vibronic origin which is in-plane polarized provides strong support for the $^1B_{2g}$ electronic assignment and the suggested b_{3u} (in-plane carbonyl bend) vibronic activity.

A 189-cm^{-1} vibration was observed in the first transition (370.0-nm region) and there assigned to a b_{3g} carbonyl wag. The assignment of the present 189-cm^{-1} band to the same non-totally symmetric vibration is doubtful because of the following reasoning. If it is true that vibronic mixing is primarily responsible for the intensity of this band (at least, the in-plane portion), the 312.0-nm peak represents a vibronic origin resultant from the activity of a non-totally symmetric mode built on the electronic origin. The likelihood of a second non-totally symmetric mode (the 189-cm^{-1} b_{3g} one) building on this *vibronic* origin is extremely small. It is more probable that the 189-cm^{-1} peak is a different non-totally symmetric, vibronically active mode built on the *electronic* origin. If the electronic origin were ~300 cm^{-1} (the approximate vibrational frequency of the b_{3u} carbonyl in-plane mode) below the 312.0-nm band, the vibrational frequency of the mode responsible for the 189-cm^{-1} peak would be ~490 cm^{-1}. It has been noted that a 490-cm^{-1} vibration is highly active in this transition with a five-membered progression seen. We have assigned this vibration to the out-of-plane b_{1u} carbonyl wag which in the first transition occurs at 308 cm^{-1}. Such a vibration built on a $^1B_{2g}$ electronic origin is predicted to be in-plane polarized, as observed. The presence of a vibration active in both an intensity gaining mechanism and in a long multi-membered progression is an unusual occurrence. But in the present molecule where excited state geometrical distortions have already been noted, it is perhaps reasonable to expect such a phenomenon. The implication of this assignment is that the excited state geometry must be distorted to either a boat (C_{2v}) form or a skewed boat (C_s) form. As can be seen from Table II, distortion to the symmetrical C_{2v} form does not scramble in-plane and out-of-plane polarizations, but further distortion to the C_s form may effect (cf. Table IV) such a scrambling. The experimental spectrum does show several shoulders in one polarization at positions where distinct bands appear in the other polarization, indicating that some further distortion to C_s is probably occurring.

Table IX. Vibrational Analysis of 312-nm Band System

Obsd frequency, cm^{-1}	Pol.	Obsd $\Delta\bar{\nu}$, cm^{-1}	Assignment, cm^{-1}	Calcd $\Delta\bar{\nu}$, cm^{-1}	$\Delta(\Delta\nu)$, cm^{-1}
(31744)			0–0		
32044	*z*	300	300	300	
32234	*xy*	490	490	490	
(32344) (sh)	*z*	600	600	600	
32536	*z*	792	300 + 490	790	+2
32700	*xy*	956	2 × 490	980	−24
32906	*z*	1162	1162	1162	0
33026	*z*	1282	1282 or 300 + 2 × 490	1280	+2
33269	*xy*	1525	300 + 1225	1525	0
33532	*z*	1788	300 + 3 × 490	1770	+18
33865	*xy*	2121	300 + 1225 + 600	2125	−4
34120	*z*	2376	300 + 4 × 490	2260	+116
34298	*xy*	2554	2 × 1282	2564	−10
34417	*xy*	2673			
34507	*z*	2763	300 + 5 × 490	2750	+13
34649 (sh)	*z*	2905			

Table IX shows that the vibrational structure in this transition can be readily understood in terms of progressions in the 490-cm^{-1} mode built on either the 312.0-nm vibronic origin or the electronic origin. One mode appearing 862 cm^{-1} above the 312.0-nm peak is assigned to a b_{3u} vibration (possibly a ring carbon–carbon stretching motion) built on the electronic origin. Its excited state frequency (~1162 cm^{-1} = 862 + 300 cm^{-1}) corresponds well with the ground state frequency (1180 cm^{-1}). Its out-of-plane polarization behavior is also correctly predicted with this assignment.

The proposal upon which the analysis of this band depends, namely, that the 490-cm^{-1} mode be assigned to the b_{1u} carbonyl out-of-plane wag, requires some justification. At first glance, this proposal may appear unreasonable since an increase to 490 cm^{-1} from a ground state frequency of 402 cm^{-1} is opposite to the decrease to 308 cm^{-1} observed in the first electronic transition. An increase in vibrational frequency signifies a narrower excited state potential surface than in the ground state, and a decrease in frequency a broader surface. Both these changes may in fact occur if there is vibronic interaction between the excited electronic states involved (in this case the two electronic $^1B_{2g}$ states). The coupling vibrations which must be totally symmetric are almost certainly the carbonyl wags active in both transitions which in the distorted geometries become totally symmetric. Hochstrasser and Marzzacco[16] have pointed out that the upper of two vibronically interacting potential surfaces becomes narrower with increased coupling and the lower becomes broader. They have also demonstrated that with such a vibronic interaction a broadening of the vibrational structure of the upper band can be expected. Thus, the observation of a vibrational progression in a 490-cm^{-1} b_{1u} carbonyl wagging mode and the marked broadening of the vibrational structure in this transition are consistent with the vibronic interaction between the two $^1B_{2g}$ $n\pi^*$ states.

In summary, the third transition is assigned to a $^1B_{2g}$ ($^1B_1$ or $^1A''$) electronic state whose intensity is primarily vibronically induced via several b_{3u} and b_{1u} vibrations. A progression in a 490-cm^{-1} mode is assigned to a carbonyl out-of-plane wag, an assignment which implies an excited state distortion to a

Table X. Vibrational Analysis of 285-nm Band System

Obsd frequency, cm^{-1}	Pol.	Obsd $\Delta\bar{\nu}$, cm^{-1}	Assignment cm^{-1}	Calcd $\Delta\bar{\nu}$, cm^{-1}	$\Delta(\Delta\nu)$, cm^{-1}
35068	*xyz*		0	0–0	
35670	*xyz*	602	(2 × 301)	602	
36306	*xyz*	1238	1238	1238	
36652	*xyz*	1584	1584	1584	
37254	*xyz*	2186	1584 + (2 × 301)	2186	0
37869	*xyz*	2801	1584 + 1238	2822	−21
38239	*xyz*	3171	2 × 1584	3168	+3
38850	*xyz*	3782	(2 × 1584) + (2 × 301)	3770	+12

boat or skewed boat geometry. Further, a vibronic interaction between the two $^1B_{2g}$ electronic states is indicated.

D. 285-nm Band System. Because of the simultaneous *xy* and *z* polarization of every vibration in this band system, an out-of-plane distortion to a C_{2h} (or C_s) geometry is indicated. As mentioned in the discussion on the 332.0-nm band system, neither crystalline site, factor group, nor vibronic mixing is capable of scrambling in-plane and out-of-plane polarizations. For an out-of-plane distortion it is expected that two or more quanta of an out-of-plane vibration should be excited. However, only one vibration (1584 cm^{-1}) is observed in more than one quantum (see Table X) and this mode can be reasonably assigned to the totally symmetric carbonyl stretching frequency. (The symmetric and antisymmetric carbonyl stretches occur at 1847 and 1748 cm^{-1}, respectively, in the ground state.[8]) The 1238-cm^{-1} mode, built on the 285.1-nm apparent origin and on the 1584-cm^{-1} vibronic origin, probably corresponds to the 1265-cm^{-1} ground state mode, assigned to either a nontotally symmetric ring stretching or methyl group vibration. To account for the out-of-plane distortion dictated by the polarization results, we conclude that the observed ~600-cm^{-1} bands correspond to two quanta of the b_{3g} out-of-plane carbonyl wag. This vibration was observed in several every-member progressions of 308 cm^{-1} in transitions to the similarly distorted second state (332.0 region). It is apparent from the Franck-Condon envelope of the present transition that the excited state potential surface is simply vertically shifted from the ground state one, so that the vibrational Franck-Condon overlap factors for odd quanta of the b_{3g} mode are expected to be very small and transition intensities to these levels negligible, as observed.

Unfortunately, the assignment of the electronic symmetry of this transition is more difficult than for the other transitions since the vibrational structure and polarization data are less informative. From Tables VIII and IV it can be seen for distortion to a C_{2h} or C_s geometry that transitions to an A_u state should be observed along *x* and that transitions to a B_{2g} state should be forbidden or polarized along *x*, respectively. The strong apparent origin at 285.1 nm is observed polarized along both *xy* and *z* directions, with the former more intense. Thus, this band must be a vibronic origin with the electronic origin somewhere to lower energy. Although no band in this region can be clearly identified as the origin band, the in-plane polarized 285.1-nm band is skewed at its red edge which might indicate the presence of the real origin underneath. None of the present data allow an unambiguous choice of electronic symmetry for this transition; however, a ^1A_u assignment can be inferred since the lower three transitions have already been assigned to one ^1A_u and two $^1B_{2g}$ transitions. Because of the strong in-plane intensity of the 285.1-nm vibronic band intensity its (C_{2h}) vibronic symmetry is B_u (cf. Table VII) of B_{1u} or B_{2u} (D_{2h}) parentage. For a ^1A_u electronic state, this suggests either b_{1g} or b_{2g} coupling vibrations. A combination b_{2g} vibration at 270 cm^{-1} has been assigned in the ground state, as have a b_{1g} in-plane carbonyl bend at 216 cm^{-1} and a b_{1g} ring distortion mode at 661 cm^{-1}. Either of the first two suggestions is consistent with the origin being slightly to lower energy of the 285.1-nm band. From the skewness and band width of the latter, it is estimated that the origin band should be between 200 to 350 cm^{-1} from the 285.1-nm peak.

Thus, the fourth transition is assigned to a ^1A_u (^1A_u or $^1A''$) state in which the excited state is out-of-plane distorted to a chair form (C_{2h}) or skewed chair form (C_s). Vibronic coupling via a low-energy mode appears to be primarily responsible for the observed in-plane intensity and valence distortion for the out-of-plane intensity. Two quanta of the totally symmetric carbonyl stretching frequency have been observed; the absence of odd quanta of the b_{3g} carbonyl wagging frequency has been deduced from the Franck–Condon envelope and polarization results of the complete transition.

VII. Discussion

On the basis of relative intensities, polarizations, and vibrational structure, the four singlet $n\pi^*$ transitions in TMCBD have been assigned, in order of increasing energy, to ^1A_u ($^1A_2$), $^1B_{2g}$ (^1B_g), $^1B_{2g}$ ($^1B_1$), and ^1A_u (^1A_u). (The symmetry assignment in the distorted molecular group is given in parentheses.) It has been further shown that the first and third electronic excited states are distorted to boat-like (C_{2v} or C_s) structures while the second and fourth states are distorted to chair-like (C_{2h} or C_s) geometries. It is apparent from the large intervals between the different $n\pi^*$ transitions that not only is there a large splitting between the nonbonding molecular orbitals (MO's) but also between the antibonding π^* MO's. In the following paper, these splittings are analyzed and calculations of the splittings attempted with several semiempirical LCAO–MO theories. Suffice it to say here that the best calculation yields an MO level ordering: $n_-(b_{1g}) < n_+(b_{3u}) < \pi_-^*(b_{3g}) < \pi_+^*(b_{1u})$. The predicted order of transitions between these MO's is as observed in this investigation, and the calculated intervals between the different $n\pi^*$ transitions reproduce the experimentally observed intervals fairly well.

To the best of our knowledge, this is the first time that four $n\pi^*$ transitions have been clearly identified in an aliphatic diketone with known ground state structure. Much other work on such interesting systems as glyoxal, biacetyl, oxalyl chloride, camphorquinone, etc. has been reported but each has been beset by difficulties such as unknown ground state conformation (cis vs. trans vs. mixture), unknown crystal structure, overlapping spectral bands, or impurity absorption. Although theoretical work has also been reported on the interaction between lone pairs in many dicarbonyls, these efforts have been handicapped by the lack of precise knowledge of all the possible $n\pi^*$ transitions. We are hopeful that the work presented here will encourage further theoretical study of the interactions between nonbonding electron pairs in diketones.

Acknowledgments. We gratefully acknowledge the National Science Foundation for support of this research through Grant No. 12740A1. We also wish to express our gratitude to Dr. H. P. Trommsdorff of the University of Grenoble for performing the Stark effect measurement and for assistance with the *ac* face polarization measurements.

References and Notes

(1) E. A. LaLancette and R. E. Benson, *J. Am. Chem. Soc.*, **83**, 4867 (1961).
(2) E. M. Kosower, *J. Chem. Phys.*, **38**, 2813 (1963).
(3) J. E. Fernandez and A. A. More, *Q. J. Fla. Acad. Sci.*, **26**, 217 (1963).
(4) R. E. Ballard and C. H. Park, *Spectrochim. Acta, Part A*, **26**, 43 (1970).
(5) J. R. Swenson and R. Hoffmann, *Helv. Chim. Acta*, **53**, 2331 (1970).
(6) D. Cowan, R. Gleiter, J. Hashmall, E. Heilbronner, and V. Hornung, *Angew. Chem.*, **10**, 401 (1971).
(7) P. H. Friedlander and J. M. Robertson, *J. Chem. Soc.*, 3080 (1956); C. Riche, *C. R. Acad. Sci. Paris*, **245**, 543 (1972); C. D. Shirrell and D. E. Williams, *Acta Crystallogr., Sect. B*, **30**, 245 (1974).
(8) F. O. Nicolaisen, O. F. Nielsen, and M. Vala, *J. Mol. Struct.*, **13**, 349 (1972).

(9) M. Vala, I Trabjerg, and E. N. Svendsen, *Acta Chem. Scand., Ser. A*, **28**, 37 (1974).
(10) R. Spafford, J. Wrobel, and M. Vala, *Mol. Phys.*, **27**, 1241 (1974).
(11) A. A. Lamola, as quoted in N. J. Turro, P. A. Leermakers, H. R. Wilson, D. C. Neckers, G. W. Byers, and G. F. Vesley, *J. Am. Chem. Soc.*, **87**, 2613 (1965).
(12) R. F. Whitlock and A. B. F. Duncan, *J. Chem. Phys.*, **55**, 218 (1971).
(13) H. P. Trommsdorff, private communication.
(14) N. J. Turro, P. A. Leermakers, H. R. Wilson, D. C. Neckers, G. W. Byers, and G. F. Vesley, *J. Am. Chem. Soc.*, **87**, 2613 (1965).
(15) Another possible mechanism for polarization scrambling involves the distortion of the excited state to a skew boat C_s geometry (cf. Table IV), in which the 308-cm^{-1} mode retains its identity as the b_{1u} carbonyl wag.
(16) R. Hochstrasser and C. Marzzacco in "Molecular Luminescence", E. C. Lim, Ed., W. A. Benjamin, New York, N.Y., 1969, p 631.

Multiple nπ* Transitions in Tetramethyl-1,3-cyclobutanedione. II. Through-Bond Effects

J. Baiardo, R. Spafford, and M. Vala*

Contribution from the Department of Chemistry, University of Florida, Gainesville, Florida 32611. *Received August 26, 1975*

Abstract: The four singlet nπ* transitions observed in the diketone tetramethyl-1,3-cyclobutanedione (TMCBD) have been analyzed theoretically. The interaction of the carbonyls' nonbonding (n) and π antibonding orbitals are discussed qualitatively in terms of "through-space" vs. "through-bond" mechanisms. Through-bond interactions are shown to be the major cause of the large n orbital splitting, confirming the previously observed photoelectron spectroscopic results. The transannular (through-space) interaction of the π antibonding orbitals, a mechanism invoked by earlier workers to explain the TMCBD solution spectrum, is shown to be dominated by a "circumannular" interaction where the π* orbitals interact with ring carbon–methyl carbon σ orbitals of the correct symmetry. Finally, it is shown that the simple extended Hückel theory gives more satisfactory results for the position, ordering, and spacing of the four nπ* states than do the more sophisticated semiempirical CNDO methods, with or without configuration interaction.

I. Introduction

There have been many studies on the interaction of nonbonding electron pairs in diketones. In the preceding paper,[1] we have presented the results of our recent investigation on the low-temperature, single-crystal, polarized absorption spectrum of tetramethyl-1,3-cyclobutanedione (TMCBD). The presence of four clearly resolved electronic singlet nπ* transitions was shown and the assignments of these transitions deduced from an analysis of vibrational structure, polarization data, and relative intensities.

In the present paper we have investigated theoretically the interaction between the two carbonyl groups in cyclobutanedione (CBD) and TMCBD. In 1970 Swenson and Hoffmann[2] predicted from extended Hückel theory (EHT) and CNDO/2 calculations that there should be a large "through-bond" interaction between the nonbonding orbitals of certain diketones. Since that time specific diketones have been sought to experimentally test this idea. Because of its relatively accurate prediction of the large n orbital splittings observed in photoelectron spectra of diketones,[3] among other molecules, the "through-bond" mechanism of interaction has been generally accepted. However, the application of this idea to the electronic absorption spectra of diketones has been hindered by experimental difficulties. Problems such as unknown crystal structure, unknown ground state conformation, impurity absorption, and overlapping spectral bands have hindered the precise location of the expected nπ* transitions.

The molecule presently under study (TMCBD) does not appear to be beset by these difficulties. Its ground state conformation and crystal structure are well characterized.[4] Its photoelectron spectrum is known and understood.[3] Its infrared and Raman spectra[5] and gas-phase vacuum ultraviolet spectrum[6,7] have been investigated, and the location and assignments of its four nπ* transitions are now known.[1]

In this paper, we have chosen to employ the EHT, CNDO/2, and CNDO/S semiempirical molecular orbital methods to investigate the carbonyls' nonbonding orbital interaction and π antibonding orbital interaction. Evidence is presented for the existence of "through-bond" interactions which influence both n and π* orbital splittings. It is also pointed out that the extended Hückel theory is superior to the CNDO/2 and CNDO/S techniques, with or without configuration interaction, in predicting the energies and relative ordering of the singlet nπ* states. Finally, some of the reasons for the EHT's better performance are discussed.

II. Computational Procedures

Calculations were performed using extended Hückel theory (EHT), CNDO/2, and CNDO/S semiempirical methods; both CNDO methods were run with and without configuration interaction (CI). Some of the approximations used in the latter two methods are discussed later. Programs were supplied by QCPE. In our calculations using EHT and CNDO/S techniques, we have investigated both CBD and TMCBD to determine the effect of the methyl groups. The geometry of CBD was taken to coincide with the planar part of TMCBD, as determined by an x-ray structure determination.[4] The C-C bonds are 1.56 Å, the C-O distances 1.20 Å, the C-H distances 1.10 Å, the C-C-C ring angles 90°, and the HCH angles 116°. The conformation of the methyl groups in TMCBD was deduced from the x-ray structure determination. The methyls across the ring and on the same side of the molecular plane are slightly skewed in opposite directions, so that the true molecular point group is D_2, and not D_{2h} as for CBD. For one EHT calculation the methyl groups were chosen eclipsed (across the ring) such